POLITECNICO DI TORINO
Repository ISTITUZIONALE

Refined annotations of intrahepatic portal and hepatic veins from thin-slice CT images

Original
Refined annotations of intrahepatic portal and hepatic veins from thin-slice CT images / Salvi, M., Gassino, R., Ranzini, M.B.M., Ferillo, G., Vacca, L., Isu, G., Orini, C., Angileri, G., Meiburger, K.M., Laghi, A.. - In: SCIENTIFIC DATA. - ISSN 2052-4463. - (In corso di stampa). [10.1038/s41597-026-08346-1]

Availability:
This version is available at: 11583/3017194 since: 2026-10-29T11:07:07Z

Publisher:
Springer

Published
DOI:10.1038/s41597-026-08346-1

Terms of use:

This article is made available under terms and conditions as specified in the corresponding bibliographic description in the repository

Publisher copyright

(Article begins on next page)

03 November 2026

scientific data

Article in Press

Check for updates

OPEN

DATA DESCRIPTOR

Refined annotations of intrahepatic portal and hepatic veins from thin-slice CT images

Matteo Salvi[1,2] ✉, Riccardo Gassino[3], Marta Bianca Maria Ranzini[3], Giuseppe Ferillo[4], Luca Vacca[2], Giuseppe Isu[2], Claudio Orini[4], Giuseppe Angileri[4], Kristen Mariko Meiburger[1] & Andrea Laghi[4]

Accurate segmentation of intrahepatic vessels in contrast-enhanced CT is limited by spatial resolution, variable contrast timing, and the complexity of peripheral vascular anatomy. Public datasets such as the Medical Segmentation Decathlon Task 08 include annotations of hepatic structures but provide incomplete delineation of small-caliber portal and hepatic veins. This work describes HVA-CT (Hepatic Venous Annotations CT), a dataset derived from the contrast-enhanced thin-slice CT volumes of the Medical Segmentation Decathlon Task 08, in which intrahepatic venous structures were re-annotated with more complete anatomical delineation. The dataset comprises refined three-dimensional segmentations of portal and hepatic venous systems generated through a structured workflow combining baseline model outputs, AI-assisted vessel branch identification, and expert review. For each case, updated venous segmentation masks, liver segmentations, and a standardized tool for intrahepatic vessel extraction are provided. The dataset is intended to support the development and evaluation of automated methods for hepatic vessel segmentation and analysis.

Background & Summary

Accurate representation of intrahepatic venous anatomy on contrast-enhanced CT plays a central role in multiple hepatobiliary applications, including surgical planning, virtual hepatectomy, computational modeling, and quantitative liver analysis[1,2]. Detailed portal and hepatic vein reconstructions assist clinicians in evaluating resectability[3–6] and estimating the future liver remnant[7]. The level of venous detail required depends on the procedure. For standard lobar or hemiliver resections, delineation of the major trunks and their first-order branches is generally sufficient. Peripheral and segmental detail becomes important in parenchyma-sparing surgery, both anatomical (segment-oriented) and non-anatomical (wedge) resections, and in the estimation of segmental future-liver-remnant territories[7]; it is also central to living-donor liver transplantation, where the drainage territory of the middle hepatic vein and its tributaries informs whether venous reconstruction is needed to avoid graft congestion[5]. Accurate peripheral anatomy also helps anticipate which branches are at risk during resection, since division of an unrecognised branch may devascularise or bleed a segment[2]. Despite their clinical relevance[8], small-caliber intrahepatic vessels remain difficult to delineate reliably on routine contrast-enhanced CT, leading to variability and partial coverage in existing annotations[9]. In parallel, a wide range of deep learning methods have been proposed for hepatic vessel segmentation[10,11], including UNet variants[12], hybrid convolution–Transformer networks[13], and structure-aware architectures such as[14]. These techniques increasingly target fine-grained vascular topology, yet systematic benchmarking remains limited by the quality and completeness of publicly available annotations[11]. Several public datasets address liver imaging, but none offers a complete representation of intrahepatic venous anatomy on clinical CT[11]. Existing resources, including 3DIRCADb[15], VascuSynth[16], and large-scale collections such as LiVS[17] or Medical Segmentation Decathlon (MSD) Task08[18,19], either cover only a few subjects, rely on synthetic data, or mainly capture major venous trunks.

[1]InVisioning* Lab, PolitoBIOMed Lab, Department of Electronics and Telecommunications, Politecnico di Torino, Corso Duca degli Abruzzi 24, 10129, Turin, Italy. [2]Medics Srl, via Avogadro 19, 10121, Turin, Italy. [3]Humanitas AI Center, IRCCS Humanitas Research Hospital, via Manzoni 56, 20089, Milan, Rozzano, Italy. [4]Department of Diagnostic and Interventional Radiology, IRCCS Humanitas Research Hospital, Via Manzoni 56 Rozzano, 20089, Milan, Italy. ✉e-mail: matteo.salvi@polito.it

Dataset	Year	Description	# volumes	CT spacing range (mm)	Labels	Vessel annotations
3D IRCADb[15]	2010	Venous phase contrast-enhanced CT for liver segmentation algorithm evaluation	22	0.56–0.96 (x,y); 1.0–4.0 (z)	Liver, tumors, vessels	Portal and hepatic veins present and separated
VascuSynth[16]	2013	Synthetic dataset for vascular tree generation and segmentation algorithm development	120	1 (x,y) 1 (z)	Vascular structures	Fully annotated vascular trees; synthetic, non-clinical data
LiVS[17]	2022	CT dataset for liver vessel segmentation	532	0.50–0.98 (x,y); 0.63–5.0 (z)	Liver, vessels	~30 slices annotated per volume; partial 3D coverage
MSD Task08[18,19]	2019	Multi-organ abdominal CT segmentation benchmark	303	0.57–0.97 (x,y); 0.8–8.0 (z)	Liver, tumors, vessels	Single "vessel" class; large trunks and proximal branches only

Table 1. Overview of publicly available CT datasets with hepatic vessel annotations.

More recently, Xu *et al.*[14] introduced multiclass reannotations of MSD Task08[18,19] that substantially improve the separation of portal and hepatic venous systems. However, like all available annotations for this dataset, these labels still show limited coverage of fine peripheral vessels in thin-slice acquisitions. Our internal benchmarking confirmed that many small intrahepatic branches visible on thin-slice Task08 scans were consistently not included in any existing public annotations.

These observations motivated the creation of HVA-CT, a refined dataset comprising all MSD Task08[18,19] volumes with thin-slice CT ($\leq$2 mm; 61 cases), selected using an objective and reproducible criterion to ensure reliable visualization and annotation of fine-caliber intra-hepatic vessels. Each case provides expert-validated portal and hepatic vein segmentations refined through a human–AI workflow: Xu *et al.*[14] labels were used as a baseline, an assistive model proposed vessel candidates, and radiologists reviewed, corrected, and completed the anatomy in a 3D interface so that only human-approved structures are included. We also release per-case liver masks generated using Totalsegmentator[20] and an open-source intrahepatic vessel extraction based on[21] to standardize evaluation. Validation shows increased vessel completeness, especially in small peripheral branches, while preserving major trunks, and reduces benchmarking bias by reclassifying many apparent "false positives" against public annotations as true vessels.

All refined masks, liver segmentations, and reference code are publicly released. CT scans from the MSD Task08[18,19] dataset are not redistributed and must be obtained from the original source (Medical Segmentation Decathlon), but the refined masks align voxel-by-voxel with the official volumes, requiring no resampling.

HVA-CT provides a complete expert-validated intrahepatic vessel annotations currently available for the widely used MSD Task08[18,19] dataset. By improving the completeness and anatomical fidelity of venous labels on thin-slice CT, this resource supports reproducible benchmarking, advances development of vessel-segmentation models, and enables more accurate quantitative and computational studies in hepatic imaging.

Overview of Existing Public Liver Vessel Datasets

Several publicly available datasets include hepatic CT imaging, but they differ substantially in resolution, annotation methodology, and the level of vascular detail. 3DIRCADb[15] provides venous-phase CT volumes with manually curated portal and hepatic veins, although it includes only a small number of patients. VascuSynth[16] generates synthetic vascular trees with complete ground-truth topology, which is useful for algorithm development but does not reflect the appearance of clinical CT data. Among larger collections, LiVS[17], and the MSD Task08[18,19] dataset all contain vessel annotations; however, these predominantly represent major venous trunks or provide only partial 3D coverage. For MSD Task08[18,19], the more recent Xu *et al.*[14] reannotations introduce separate portal and hepatic vein labels and improve vessel-system separation.

Table 1 summarizes the main characteristics of these datasets, while Fig. 1 illustrates representative examples from datasets with complete 3D vessel annotations, highlighting differences in image resolution, vascular detail, and annotation completeness.

Methods

Source Dataset. All imaging data were obtained from the MSD Task08[18,19] dataset, which provides anonymized portal venous phase contrast-enhanced abdominal CT scans and associated organ and vessel labels. Task08 includes 303 subjects acquired across multiple institutions, with substantial variability in slice thickness and scanner protocols[22].

For this work, we selected all Task08 volumes exhibiting thin-slice axial spacing ($\leq$2 mm). Thin-slice spacing was the sole inclusion criterion, and was determined from the z-spacing reported in the original NIfTI headers. These acquisitions provide more reliable visualization of fine intrahepatic branches and are therefore suitable for detailed venous annotation. In total, 61 volumes met this requirement. All CT scans were used in their native voxel grid, preserving the original orientation, spacing, metadata, and intensity distribution provided by the Decathlon organizers.

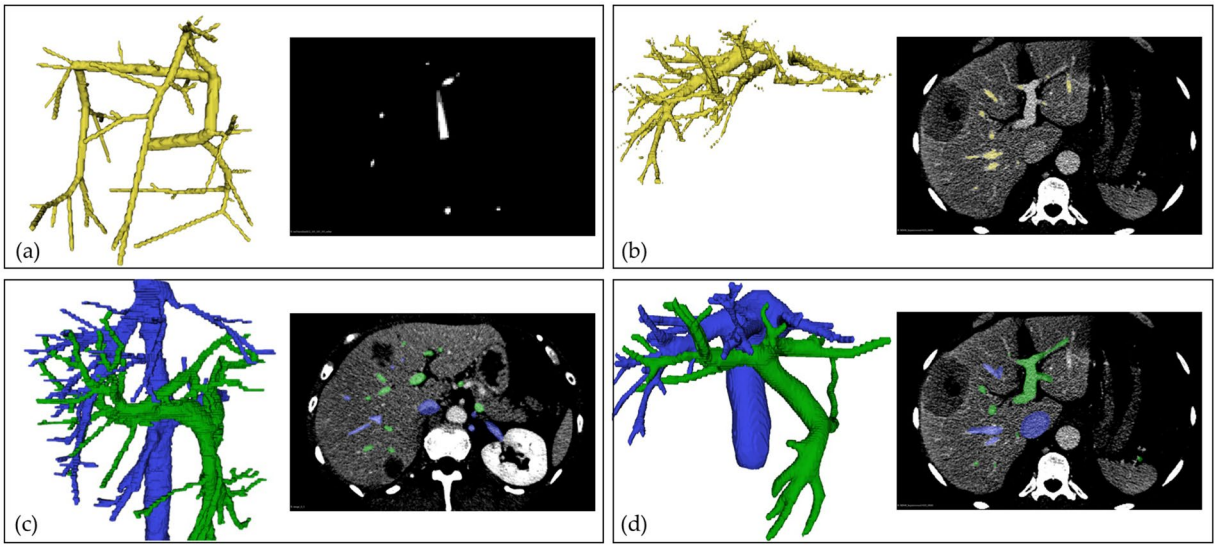


Fig. 1 Representative examples from publicly available liver vessel datasets. For each dataset, a CT slice and the corresponding 3D vessel rendering illustrate differences in annotation style and vascular detail across VascuSynth (**a**), MSD Task08 initial labels (**b**), 3DIRCADb (**c**), and Xu *et al.*[14] reannotations of the same MSD case (**d**), with single-class vessel annotations in yellow, hepatic veins shown in blue and portal veins in green.

The original CT images are not redistributed in this release and must be downloaded from the official Task08 repository.

Initial Vessel Annotations. The starting point for refinement consisted of the publicly available Xu *et al.*[14] multiclass vessel annotations for Task08, distributed under an open license and available at VSNet/reannotated.zip at main · XXYZB/VSNet. These annotations provide separate labels for the portal and hepatic venous systems and were used as structured but incomplete baseline masks. While this annotations improves venous system separation relative to the original Task08 labels, many peripheral intrahepatic branches remain incomplete due to interpretation challenges on CT (Fig. 2). In our workflow, Xu *et al.*[14] masks served solely as the initial anatomical scaffold for expert review.

Internal Model for Candidate Vessel Detection. An internal vessel segmentation model developed by Medics Srl (Turin, Italy) was used to assist the annotation workflow by identifying regions that might contain additional portal or hepatic vessels not present in the baseline labels. The model is based on a 3D U-Net architecture and produces three output classes (background, portal vein, hepatic vein). Its predictions were used only as visual cues to help annotators locate structures of potential interest during review. The model did not modify any label automatically, and all included vessels originate exclusively from expert assessment.

Overview of the Human–AI Collaborative Workflow. The refinement of the vessel annotations followed a structured human–AI workflow designed to increase the completeness of intrahepatic branches while preserving full expert control over the final labels (Fig. 3). Each case was reviewed starting from the Xu *et al.*[14] baseline masks.

Radiologists then reviewed the vessel tree using a custom visualization interface that displayed both the initial mask and any candidate vessel-like regions identified by the assistive model. Candidate segments were shown only where the initial annotation lacked vessels and were treated strictly as suggestions. During the refinement process, annotators examined each candidate region and determined whether to accept, adjust, or discard it based on the CT appearance. Experts could also add new branches manually when visible vessels were absent from both the initial label and the candidate set. All decisions were based solely on radiological assessment, and no model output was included without explicit expert verification. This workflow ensured that the refined dataset captures fine-scale intrahepatic vessels while maintaining a consistent and expert-driven annotation standard across all 61 cases.

Annotation Interface and Experts Protocol. The refined annotations were produced in two stages: independent annotation by two radiologists, followed by adjudication by a senior radiologist. Both stages were carried out in a custom 3D Slicer[23] module providing synchronized 2D and 3D visualization of the CT volume, the initial vessel masks, and AI-proposed candidate branches.

In the annotation stage, working on one venous system at a time (Fig. 4a), annotators used voxel-level tools (brush and eraser) and a tube-drawing tool that added vessels along their course without slice-by-slice delineation, and could reassign mislabeled voxels between the portal and hepatic classes. The brush and eraser worked

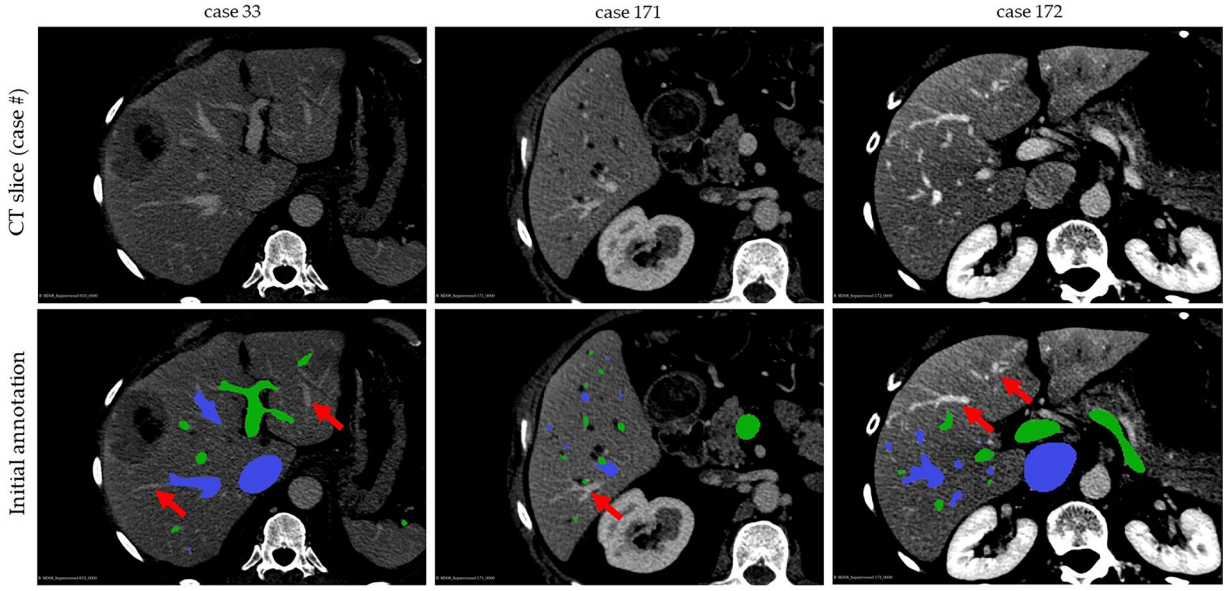


Fig. 2 Initial annotations for three representative cases. Top: CT images. Bottom: initial vessel masks with red arrows marking peripheral branches visible on CT but missing in the initial labels, motivating the refinement workflow.

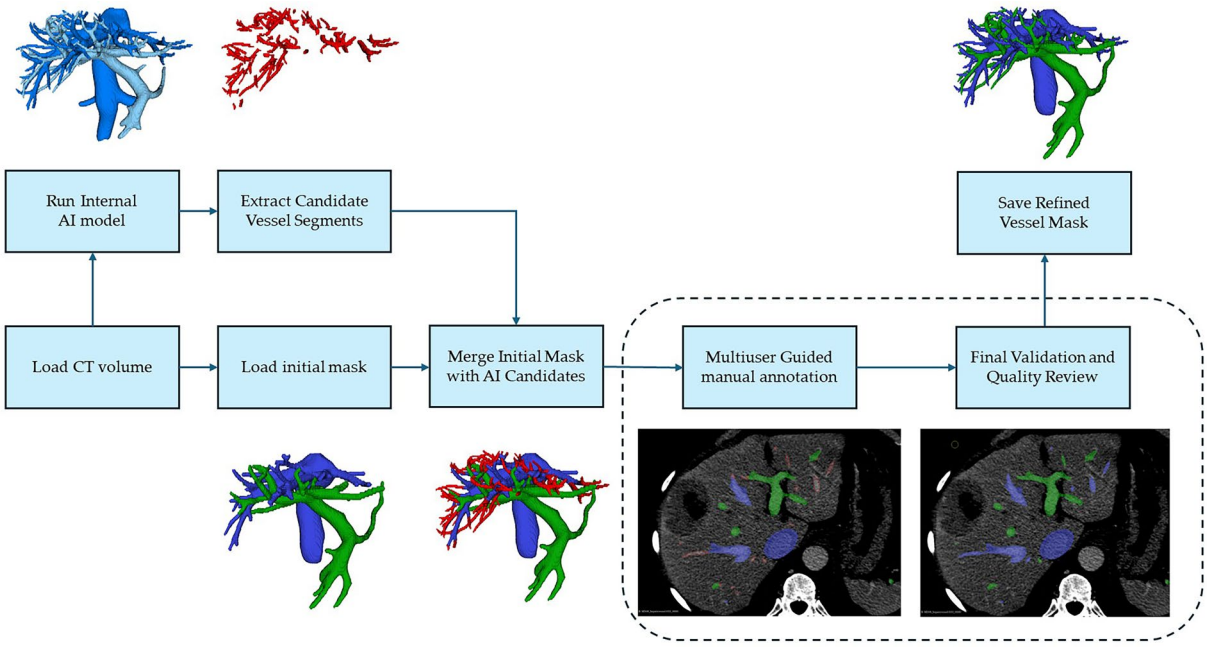


Fig. 3 Refinement workflow. Automated steps include AI-based candidate generation and mask merging. The dashed region highlights the manual radiologist-driven steps (guided refinement and expert validation) leading to the final refined vessel mask.

in both the 2D and 3D views, either restricted to the candidate regions or applied freely across the volume, so annotators were not confined to the AI-suggested areas. Because refinement started from candidates rather than a blank volume, annotation effort was concentrated on verification and correction rather than on locating and tracing peripheral vessels from scratch.

In the adjudication stage, the senior radiologist viewed both readers' annotations together, with all voxels labeled differently by the two readers highlighted in pink (Fig. 4b). The senior resolved each disagreement by removing these voxels or assigning them to the portal or hepatic class, and performed a final review of the complete mask to confirm its overall anatomical consistency.

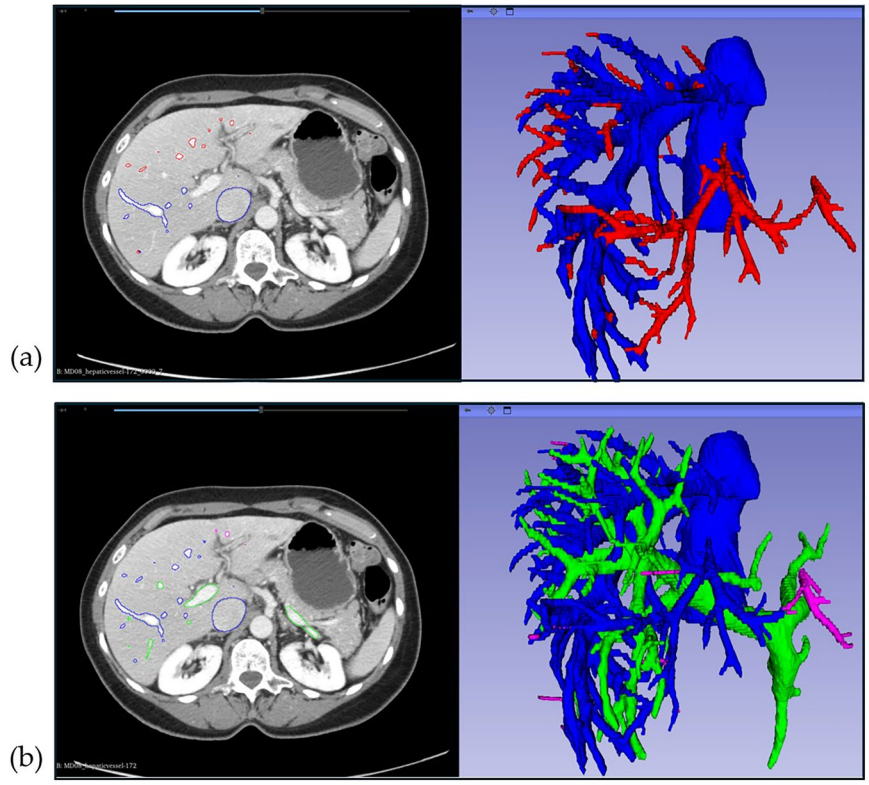


Fig. 4 Annotation and adjudication views. (**a**) Annotator view: each reader edits one venous system at a time on synchronized 2D and 3D displays; the vessel class being edited (here hepatic veins, in blue) is shown together with AI-proposed candidate branches in red. (**b**) Adjudication view: the senior radiologist sees both readers' annotations together, with disagreeing voxels highlighted in pink for resolution.

Annotators. Annotations were performed by two radiologists from Humanitas University, each with 3 years of experience in abdominal imaging. Both routinely interpret liver CT examinations and are familiar with hepatic vascular anatomy and preoperative planning workflows. All cases were annotated independently by the two readers; disagreements were resolved by a senior abdominal radiologist, blinded to reader identity, who also reviewed each mask for overall consistency (as described above).

Annotation Guidelines. Annotators followed a written protocol that required labeling all CT-visible intra-hepatic branches of the portal and hepatic venous systems. Extra-hepatic structures and non-vascular elements were excluded. For faint, low-contrast, or otherwise ambiguous vessels, a branch was labeled only when it satisfied the following criteria: (i) it was clearly traceable across contiguous slices; (ii) it showed anatomical continuity with a parent vessel of the same system rather than appearing as an isolated fragment; and (iii) its appearance was consistent with an enhancing vessel and distinguishable from imaging artifact, partial-volume blurring, or adjacent parenchymal structures. Candidates that could not be confidently attributed to a vessel were left unlabeled, favoring specificity over completeness in ambiguous regions. Automated structural checks flagged discontinuities or isolated fragments for review. Final masks represent the union of: (i) initial vessels (Xu *et al.*[14]) retained after review, (ii) accepted or corrected AI-proposed segments, and (iii) manually added vessels.

Liver Mask Generation. To provide a consistent anatomical boundary for downstream analyses, liver masks were independently generated from the original MSD Task08[18,19] images using TotalSegmentator (v2.12.0)[20]. These masks were not part of the vessel-annotation workflow described above; instead, they are released as complementary data and are later used to define the intra-hepatic region required for the vessel-extraction procedure described below.

Each mask underwent a brief visual check for large missing or spurious regions, such as an absent liver lobe, extensive inclusion of adjacent organs, or coverage of only part of the parenchyma. No such cases were identified, and no manual corrections were applied, preserving reproducibility.

The final liver masks are included in the public release and remain voxel-wise aligned with the original MSD Task08 volumes.

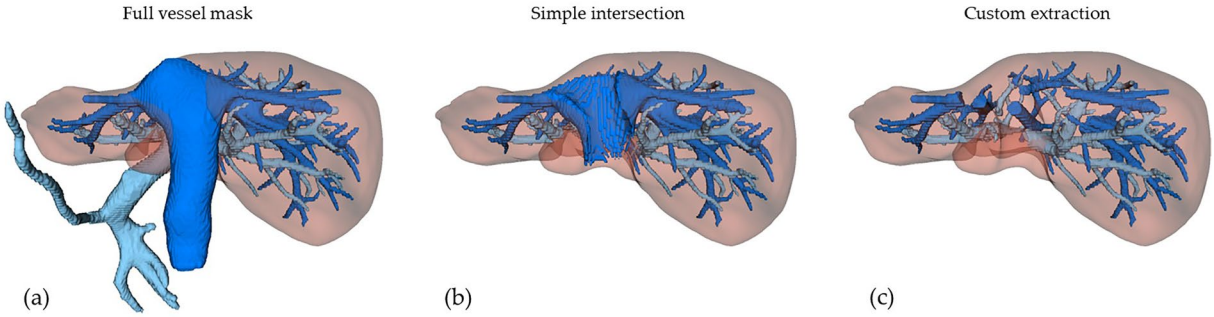


Fig. 5 Comparison of intra-hepatic extraction strategies. (**a**) Full portal (light blue) and hepatic (blue) vessel mask visualized with the liver surface (light red). (**b**) Simple vessel–liver intersection, which truncates parenchymal branches and retains parts of the extra-hepatic trunk. (**c**) Proposed extraction method, which removes the extra-hepatic trunk while preserving intra-hepatic vessels.

Intra-Hepatic Vessel Extraction Tool. To ensure consistent evaluation across cases, we provide a standardized tool that isolates the intra-hepatic portions of the portal and hepatic venous trees. The extraction relies on the TotalSegmentator liver mask to define the parenchymal region (see Liver Mask Generation), addressing the limitations of simple vessel–liver intersections, which often truncate peripheral branches or retain parts of the extra-hepatic trunk (Fig. 5). Using an automated liver mask also avoids additional manual delineation and ensures a reproducible intrahepatic boundary across all subjects.

For each venous class, the extraction procedure, adapted from the strategy used in[21], consists of:

1. **Erosion** of the vessel mask *d times* ($3 \times 3 \times 3$ structuring element) to obtain a compact representation dominated by the proximal trunk.
2. **Identification** of the largest connected component, corresponding to the extra-hepatic trunk.
3. **Dilation** of this component (same structuring element, repeated $d + 2$ iterations) to approximate the spatial extent of the extra-hepatic region.
4. **Intra-hepatic definition**:

$$intrahepatic_class = (vessels_mask \bigcap liver_mask) \backslash dilated_trunk$$

5. **Optional removal of small isolated components** below a user-defined threshold (e.g., <5 voxels).

This procedure is applied identically to the initial masks, the refined annotations, and all model predictions used in technical validation. The implementation is publicly available to ensure reproducible intra-hepatic evaluation.

Vessel Morphometrics. The initial and refined annotations were characterized using four vessel morphology metrics: vessel volume, skeleton length, branch count and vessel radius. All four were computed identically for every mask, so that initial and refined annotations are directly comparable. Vessel volume was computed as the number of labeled voxels multiplied by the physical voxel volume, yielding volumes in mm^3. The vessel skeleton was obtained by 3D morphological thinning (skeletonize from scikit-image[24]). Skeleton length was calculated as the total physical length of this centerline, obtained by summing the physical distances between adjacent skeleton voxels (26-connectivity), scaled by the voxel spacing, and reported in millimeters. Branching complexity was assessed from the skeleton topology: branch points were identified as skeleton voxels with three or more neighbors, and the branch count was defined as the number of connected skeleton segments remaining after branch-point removal. Vessel radius was estimated from the Euclidean distance transform of the vessel mask (distance_transform_edt from SciPy[25]), accounting for voxel spacing, with local radii sampled at the skeleton voxels and reported in millimeters; All computations were performed in Python using scikit-image[24] and SciPy[25] and are available in the released code (see Code Availability).

Ethics Statement. This work uses only publicly available, fully anonymized CT volumes from the Medical Segmentation Decathlon (Task08)[18,19]. No new patient data were collected. All annotations were performed on de-identified images in compliance with the data license and without access to patient-identifying information.

Because the study consists solely of re-annotation and redistribution of labels for an openly available dataset, it does not constitute human-subjects research and did not require approval from an ethics committee. Radiologists from Humanitas contributed exclusively to image annotation and quality control and had no access to personal health information. All refined annotations and associated tools are released under an open license (CC BY-SA 4.0) to support reproducibility and community use.

Data Records

All refined vessel annotations generated in this study are publicly available on Zenodo[26] under the (https://doi.org/10.5281/zenodo.19850108). The release includes expert-validated portal and hepatic vein masks, liver segmentations, and minimal metadata required for reproducible use. The original CT scans from the MSD Task08[18,19] are not redistributed and must be obtained separately from Medical Segmentation Decathlon. The dataset follows the directory structure below:

Folder	Format	Description
hp_masks/	.nii.gz	Refined 3D venous annotations (portal = 1, hepatic = 2).
liver_masks/	.nii.gz	Companion liver masks generated with TotalSegmentator.
metadata/	.json	Image and annotations metadata
task08_case_list/	.txt	List of MSD Task08 included cases.

All files are voxel-wise aligned with the corresponding Task08 CT volumes and require no resampling.

Metadata File. A single JSON file (metadata.json) summarizes key properties for all 61 cases. For each subject, the file includes:

Category	Field name	Description
Acquisition metadata	case_id	Original Task08 subject identifier.
	spacing_x, spacing_y, spacing_z	Physical voxel spacing in millimeters.
	dim_x, dim_y, dim_z	Image dimensions (number of voxels).
Annotation metadata	portal_voxels	Number of voxels labeled as portal veins.
	hepatic_voxels	Number of voxels labeled as hepatic veins.
	vessel_voxels_total	Total number of venous voxels (portal + hepatic).
	liver_voxels	Number of voxels included in the liver mask.
	portal_skeleton_length_mm	Length of the portal vein skeleton in millimeters.
	hepatic_skeleton_length_mm	Length of the hepatic vein skeleton in millimeters.

This metadata file allows users to easily explore acquisition variability, stratify analyses, and design preprocessing pipelines without manually parsing individual NIfTI headers.

Technical Validation

We assessed the refined annotations along two axes: their reliability, established through inter–observer agreement between the two independent radiologists, and the anatomical improvement they provide, quantified through structural and topological metrics before and after refinement. Complete structural and class-specific analyses were computed on the full vessel masks, while the intra-hepatic analyses were performed after trunk removal using the standardized extraction method described above. The pre-refinement annotations are those of Xu *et al.*[14], which are, to our knowledge, the most complete publicly available portal/hepatic labeling of MSD Task08[18,19]; because HVA-CT refines these same masks on the same images, the metrics reported below constitute a direct, voxel-aligned quantitative comparison against the current state-of-the-art public annotation. A visual example of the initial and refined vessel masks is provided in Fig. 6.

Inter–observer Agreement. The reliability of the refined annotations was assessed by comparing the two radiologists' independent annotations before senior adjudication. Because both readers started from and preserved a shared baseline mask, agreement computed over the full mask is dominated by unchanged voxels and overstates concordance. We therefore restricted the comparison to the refined region, the voxels each reader added or modified relative to the baseline, which reflects the annotation decisions actually made during refinement. Agreement in this region was high: the median Dice was 0.991 for both the portal (IQR 0.976–0.997) and hepatic (IQR 0.978–0.997) venous systems, and pooled agreement gave a Cohen's κ of 0.948.

Most cases showed near-perfect overlap, and the disagreements that did occur were concentrated in a small number of cases. These fell into two categories. Most concerned which vessels to include: short terminal or peripheral branches identified by only one reader, or small boundary differences. A second, less frequent category concerned the portal or hepatic label itself: in 19 of 61 cases the two readers assigned different labels to some voxels. These label disagreements are the more consequential kind, because the portal or hepatic label determines which venous system a vessel belongs to, and an incorrect label can make the local anatomy implausible. All disagreements were resolved by a senior abdominal radiologist, blinded to reader identity, who assigned a single, anatomically consistent labeling; the adjudicated masks form the released annotations. Figure 7 shows a representative case, illustrating disagreements from terminal-branch detection, boundary variation, and label assignment, together with the adjudicated mask.

Structural Comparison Across Annotation Sets. Structural metrics computed on the full vessel masks show that the refined annotations recover additional intra-hepatic branches while preserving the overall vascular architecture. Table 2 reports increases in vessel volume, skeleton length, and branching complexity, with the largest relative gains observed in topology-sensitive measures. The relatively small increase in vessel volume is

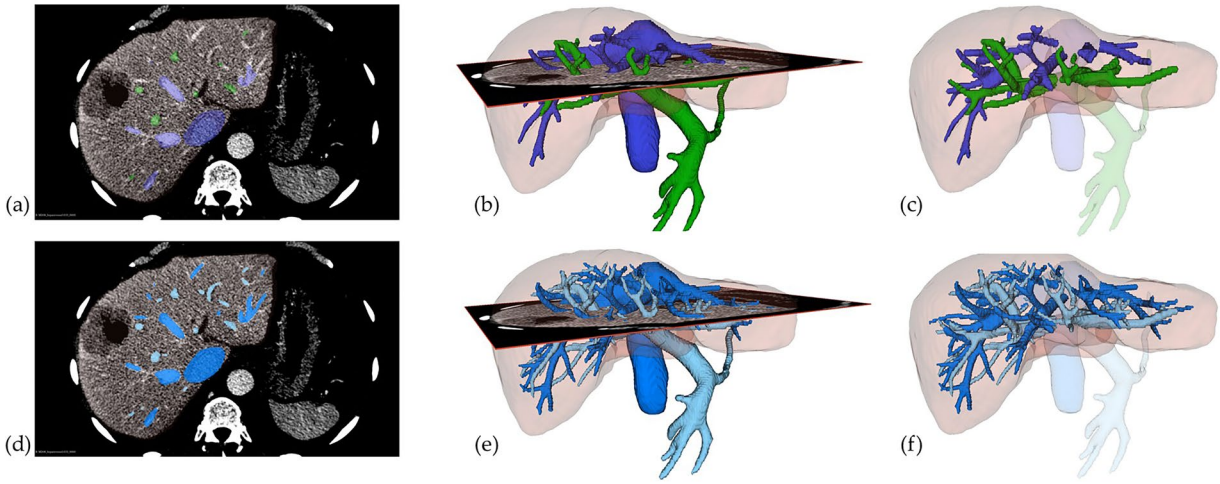


Fig. 6 Initial and refined vessel annotations for a representative MSD Task08 case. (**a–c**) Initial annotations of portal (green) and hepatic (blue) veins shown as a CT slice, full 3D vessel mask, and intra-hepatic vessels after trunk removal in an alternative 3D view. (**d–f**) Corresponding portal (light blue) and hepatic (dark blue) refined annotations, illustrating increased branch completeness and improved intra-hepatic detail.

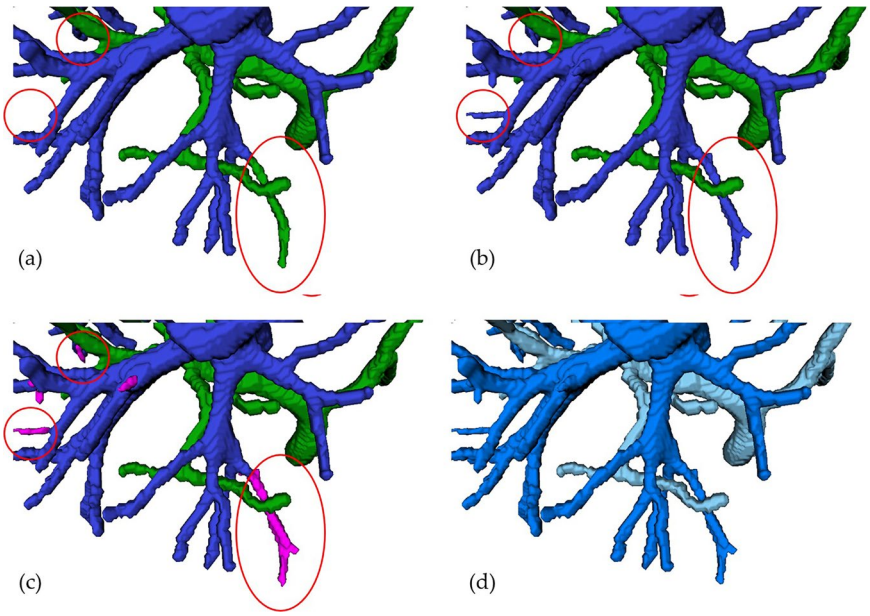


Fig. 7 Inter-observer comparison and senior adjudication for a representative case. (**a,b**) Independent annotations from radiologist 1 and radiologist 2, with portal veins in green and hepatic veins in blue; red circles mark disagreements. (**c**) Overlay of both annotations, with differing voxels in pink and the same regions circled. (**d**) Senior-adjudicated mask (the released annotation), with portal veins in light blue and hepatic veins in dark blue.

expected, as the refinement process primarily adds thin peripheral branches that contribute little to total volume but substantially increase skeleton length. To further localize where these differences occur, Fig. 8 shows the distribution of skeleton voxels across radius bins. The refined masks exhibit clear improvements in the small-radius range (0–2 mm), corresponding to thin peripheral vessels that were only partially captured in the initial annotations, while medium- and large-radius bins remain nearly unchanged, confirming preservation of major venous structures. All reported differences between initial and refined metrics were statistically significant (Wilcoxon signed-rank test, $p < 0.001$).

Class-Specific Improvements (Portal vs Hepatic Veins). Portal and hepatic veins were analyzed separately using the full vessel masks. Both venous systems exhibit comparable improvements following refinement, with increases in skeleton length, branch counts, and enrichment of small-radius branches (Table 3).

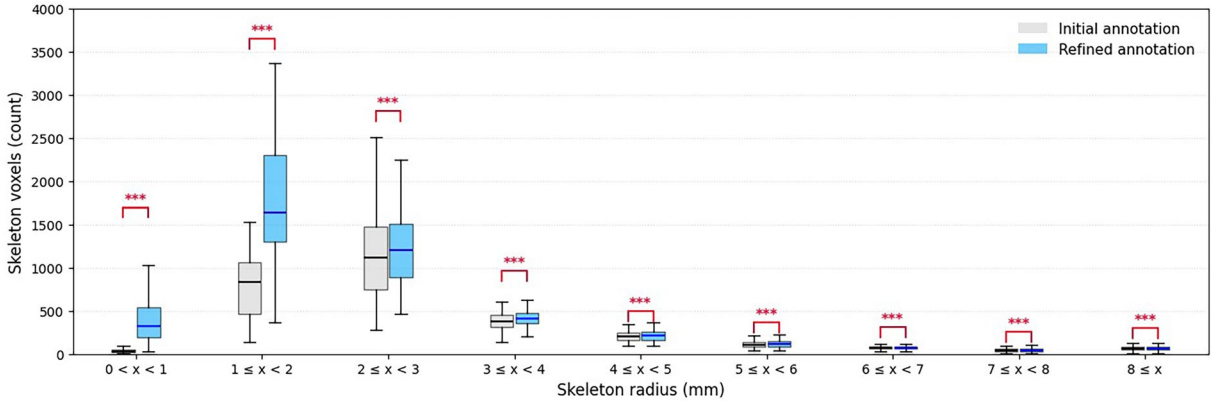


Fig. 8 Skeleton voxel counts across radius bins for the initial (gray) and refined (light blue) annotations. Paired boxplots represent the per-subject distribution within each radius interval. The refined annotations show significantly increased counts in the smaller radius bins (0–2 mm), indicating improved recovery of thin peripheral branches (***$p < 0.001$).

Metric	Initial dataset (mean ± SD)	Reannotations (mean ± SD)	Δ mean (%)
Vessel volume [mm³]	157782 ± 33599	168707 ± 33873	+6.92
Skeleton length [mm]	3954 ± 1260	5752 ± 1545	+45.47
Branch count	188 ± 76	296 ± 94	+57.82

Table 2. Structural and topological metrics for the initial and refined vessel annotations across all 61 cases (full masks). Mean ± standard deviation are reported for each metric, together with the relative change in the mean after refinement (Δ mean %).

	Metric	Initial dataset (mean ± SD)	Reannotations (mean ± SD)	Δ mean (%)
Portal	Vessel volume [mm3]	58495 ± 18296	62649 ± 18491	+7.10
Hepatic	Vessel volume [mm3]	99287 ± 23223	106057 ± 23871	+6.82
Portal	Skeleton length [mm]	1834 ± 756	2607 ± 848	+42.18
Hepatic	Skeleton length [mm]	2120 ± 667	3145 ± 939	+48.33
Portal	Branch count	81 ± 42	128 ± 52	+57.15
Hepatic	Branch count	106 ± 45	168 ± 62	+58.33

Table 3. Class-specific structural metrics for portal and hepatic veins before and after refinement. Mean ± standard deviation are reported for each metric, together with the relative change in the mean (Δ mean %).

Both venous systems show comparable patterns of refinement, indicating consistent improvements across portal and hepatic vessels.

Intra-Hepatic Analysis After Trunk Removal. To evaluate differences restricted to the parenchymal vasculature, we repeated the analysis on the intra-hepatic vessels only, obtained after applying the trunk-removal procedure (see Intra-Hepatic Vessel Extraction Tool). Within this region, the effects of refinement are more pronounced. As shown in Table 4, intra-hepatic vessel volume, skeleton length, and branch counts all increase, reflecting improved recovery of distal branches. Notably, the volume increase is more substantial than in the full-mask analysis, because removing the large extra-hepatic trunk eliminates a dominant structure that remains unchanged across both annotation sets; as a result, the contribution of the newly recovered peripheral branches becomes more apparent.

Consistency Check. As a supporting check, complementing the annotation workflow and the analyses above, we assessed whether the refined annotations are coherent with vessels predicted by a separate segmentation model. An additional vessel segmentation model was used solely as a diagnostic tool to compare prediction overlap with the initial and refined annotations; the results should not be interpreted as an evaluation of model performance.

Within the intrahepatic region, predictions showed higher spatial agreement with the refined labels than with the initial annotations (Table 5), with precision increasing from 0.764 to 0.962. This indicates that many structures previously counted as false positives against the initial labels correspond to vessels now included in the refined dataset. This supports the internal consistency of the refined annotations rather than assessing model performance.

Metric	Initial dataset (mean ± SD)	Reannotations (mean ± SD)	Δ mean (%)
Vessel volume [mm³]	46823 ± 17865	57324 ± 16054	+22.43
Skeleton length [mm]	2736 ± 1121	4371 ± 1299	+59.77
Branch count	145 ± 65	241 ± 83	+66.59

Table 4. Structural and topological metrics restricted to the intra-hepatic vessels after trunk removal. Mean ± standard deviation are reported for the initial and refined annotations, together with the relative change in the mean (Δ mean %).

Metric	Initial dataset (mean ± SD)	Reannotations (mean ± SD)
Dice score	0.671 ± 0.074	0.782 ± 0.089
Precision	0.764 ± 0.138	0.962 ± 0.023
Recall	0.632 ± 0.121	0.671 ± 0.128

Table 5. Overlap metrics from an independent segmentation model, comparing agreement with the two annotation sets. Values (mean ± SD) represent averages across the portal and hepatic classes.

Usage Notes

The refined vessel masks are released in NIfTI format and are voxel-wise aligned with the original MSD Task08[18,19] CT volumes. Users should download the corresponding CT scans from the Medical Segmentation Decathlon repository and can load the masks directly without resampling or reorientation.

An optional tool is included for extracting the intrahepatic portions of the vessel trees using the liver masks provided. Applying this step is recommended when computing intrahepatic metrics or comparing model predictions to the refined annotations, as it removes extrahepatic trunks and yields a consistent definition of the parenchymal vasculature.

Potential use cases include training or evaluating vessel segmentation models, computing vascular topology descriptors, and performing quantitative liver analyses that depend on portal or hepatic venous anatomy. Several characteristics should be taken into account when reusing this dataset. The annotations represent vessels visible on contrast-enhanced CT and are intended as an imaging reference rather than anatomical ground truth; vessels below the resolution or contrast threshold of the acquisition are not represented. The dataset comprises 61 cases from a single source (MSD Task08) and was restricted to thin-slice acquisitions ($\leq$2 mm), a choice made to maximize the visibility and annotation fidelity of fine peripheral vessels, which are less resolvable at coarser slice spacing. It is therefore not representative of the full range of clinical slice thicknesses. Models trained on it are expected to be most reliable on thin-slice data and to degrade under the domain shift introduced by thicker-slice acquisitions, where increased partial-volume averaging lowers vessel–parenchyma contrast, with the smallest peripheral branches being the most affected.

Data availability

All refined venous annotations, companion liver masks, metadata, and case lists generated in this study are publicly available on Zenodo under the dataset: https://doi.org/10.5281/zenodo.19850108.

The release includes expert-validated portal and hepatic vein masks (hp_masks.zip), liver masks generated with TotalSegmentator (liver_masks.zip), subject-level metadata (metadata.json), and the full list of included MSD Task08 cases (task08_case_list.txt).

The original CT images from the Medical Segmentation Decathlon Task08 are not redistributed and must be obtained separately through the MSD repository (http://medicaldecathlon.com/).

Code availability

All code used for intra-hepatic vessel extraction, structural metric computation, and segmentation metric evaluation, is provided as part of the dataset (https://doi.org/10.5281/zenodo.19850108)[26] in the HVA_CT_accompaning_code.zip file. The 3D Slicer annotation module used during dataset refinement is proprietary and not required to reproduce the final labels. For this reason, it is not part of the public release. All refined vessel masks and all tools required for evaluation are freely provided.

Received: 29 April 2026; Accepted: 14 September 2026;
Published: xx xx xxxx

References

1. Le, D. C., Chansangrat, J., Keeratibharat, N. & Horkaew, P. Functional Segmentation for Preoperative Liver Resection Based on Hepatic Vascular Networks. *IEEE Access* **9**, 15485–15498 (2021).
2. Iqbal, S., Iqbal, R. & Iqbal, F. Surgical Implications of Portal Vein Variations and Liver Segmentations: A Recent Update. *J. Clin. Diagn. Res. JCDR* **11**, AE01–AE05 (2017).
3. Seyama, Y. & Kokudo, N. Assessment of liver function for safe hepatic resection. *Hepatol. Res. Off. J. Jpn. Soc. Hepatol.* **39**, 107–116 (2009).

4. Ruzzenente, A. *et al*. Hyper accuracy three-dimensional (HA3D^{TM}) technology for planning complex liver resections: a preliminary single center experience. *Updat. Surg.* **75**, 105–114 (2023).
5. Mise, Y. *et al*. Virtual liver resection: computer-assisted operation planning using a three-dimensional liver representation. *J. Hepato-Biliary-Pancreat. Sci.* **20**, 157–164 (2013).
6. Felli, E. *et al*. Paradigm shift: should preoperative 3D reconstruction models become mandatory before hepatectomy for hepatocellular carcinoma (HCC)? Results of a multicenter prospective trial. *HPB* **25**, 293–300 (2023).
7. Milana, F. *et al*. How Much Is Enough? A Surgical Perspective on Imaging Modalities to Estimate Function and Volume of the Future Liver Remnant before Hepatic Resection. *Diagnostics* **13**, 2726 (2023).
8. Jiang, J., Pei, L. & Jiang, R. Clinical efficacy and safety of 3D vascular reconstruction combined with 3D navigation in laparoscopic hepatectomy: systematic review and meta-analysis. *J. Gastrointest. Oncol.* **13**, 1215–1223 (2022).
9. Ciecholewski, M. & Kassjański, M. Computational Methods for Liver Vessel Segmentation in Medical Imaging: A Review. *Sensors* **21**, (2021).
10. Delmoral, J. C. & R. S. Tavares, J. M. Semantic Segmentation of CT Liver Structures: A Systematic Review of Recent Trends and Bibliometric Analysis. *J. Med. Syst.* **48**, 97 (2024).
11. Sethia, K. *et al*. Advances in liver, liver lesion, hepatic vasculature, and biliary segmentation: a comprehensive review of traditional and deep learning approaches. *Artif. Intell. Rev.* **58**, 299 (2025).
12. Yu, W. *et al*. Liver Vessels Segmentation Based on 3 d Residual U-NET. in *2019 IEEE International Conference on Image Processing (ICIP)* 250–254 https://doi.org/10.1109/ICIP.2019.8802951 (2019).
13. Xu, J. *et al*. Hepatic and portal vein segmentation with dual-stream deep neural network. *Med. Phys.* **51**, 5441–5456 (2024).
14. Xu, J. *et al*. VSNet: Vessel Structure-aware Network for hepatic and portal vein segmentation. *Med. Image Anal.* **101**, 103458 (2025).
15. 3D-IRCADb-01. *IRCAD* https://www.ircad.fr/research/data-sets/liver-segmentation-3d-ircadb-01/ (2010).
16. Hamarneh, G. & Jassi, P. VascuSynth: Vascular tree synthesis and volumetric image generation. *VascuSynth* http://vascusynth.cs.sfu.ca/ (2013).
17. Liang Z. Liver Vessel Segmentation. *IEEE DataPort* https://doi.org/10.21227/rwys-mk84 (2022).
18. Medical Segmentation Decathlon: Task08 Hepatic Vessel. *Amazon Web Services Open Data* https://msd-for-monai.s3-us-west-2.amazonaws.com/Task08_HepaticVessel.tar (2021).
19. Antonelli, M. *et al*. The Medical Segmentation Decathlon. *Nat. Commun.* **13**, 4128 (2022).
20. Wasserthal, J. *et al*. TotalSegmentator: robust segmentation of 104 anatomical structures in CT images. *Radiol. Artif. Intell.* **5**, e230024 (2023).
21. Zheng, S., Zhang, T., Zhuang, J., Wang, H. & Liu, J. A Two-Stream Meticulous Processing Network for Retinal Vessel Segmentation. Preprint at https://doi.org/10.48550/arXiv.2001.05829 (2020).
22. Simpson, A. L. *et al*. A large annotated medical image dataset for the development and evaluation of segmentation algorithms. Preprint at https://doi.org/10.48550/arXiv.1902.09063 (2019).
23. Fedorov, A. *et al*. 3D Slicer as an image computing platform for the Quantitative Imaging Network. *Magn. Reson. Imaging* **30**, 1323–1341 (2012).
24. Walt, Svander *et al*. scikit-image: Image processing in Python. *PeerJ* **2**, e453 (2014).
25. Virtanen, P. *et al*. SciPy 1.0: fundamental algorithms for scientific computing in Python. *Nat. Methods* **17**, 1–12 (2020).
26. Salvi, M. *et al*. HVA-CT: Hepatic Venous Annotations CT. https://doi.org/10.5281/zenodo.19850108 (2026).

Acknowledgements

The authors thank Alice Ciallella and Raffaella d'Arienzo for their technical advice and domain expertise, which informed the development of the data annotation tool used in this work.

Author contributions

M.S. designed the study, developed the annotation and processing pipeline, implemented the extraction tools, curated and handled the data, and drafted the manuscript. R.G. co-designed and implemented the processing pipeline with M.S., contributed to methodology development, and assisted in organizing the manuscript structure. G.I. and L.V. contributed to data handling, internal tool support, and quality assurance during the refinement process. G.F., G.A., and C.O. performed the vessel annotations, refined the annotation guidelines, and conducted radiological validation of the final masks. M.R. contributed to the annotation process, refined the annotation guidelines, facilitated coordination between Medics and Humanitas, and provided substantive feedback on the manuscript. K.M.M. and A.L. jointly supervised the study. K.M.M. supervised the computational and methodological aspects of the study, while A.L. supervised the radiological aspects and contributed to manuscript revision. All authors contributed to the interpretation of the data and approved the final version of the manuscript.

Funding

The authors declare that no external funding was received for the research. Publication of this work was supported by Politecnico di Torino.

Competing interests

Medics Srl (Turin, Italy) developed the annotation interface and AI based tools used to support candidate vessel identification during dataset creation, and some authors are employees of the company. The company's role was limited to the development of annotation tools and workflows. All final vessel annotations and dataset curation decisions were performed by independent expert radiologists. The authors declare no other competing interests.

Additional information

Correspondence and requests for materials should be addressed to M.S.

Reprints and permissions information is available at www.nature.com/reprints.

Publisher's note Springer Nature remains neutral with regard to jurisdictional claims in published maps and institutional affiliations.

Open Access This article is licensed under a Creative Commons Attribution-NonCommercial-NoDerivatives 4.0 International License, which permits any non-commercial use, sharing, distribution and reproduction in any medium or format, as long as you give appropriate credit to the original author(s) and the source, provide a link to the Creative Commons licence, and indicate if you modified the licensed material. You do not have permission under this licence to share adapted material derived from this article or parts of it. The images or other third party material in this article are included in the article's Creative Commons licence, unless indicated otherwise in a credit line to the material. If material is not included in the article's Creative Commons licence and your intended use is not permitted by statutory regulation or exceeds the permitted use, you will need to obtain permission directly from the copyright holder. To view a copy of this licence, visit http://creativecommons.org/licenses/by-nc-nd/4.0/.

© The Author(s) 2026

This Article in Press is shared early to give you faster access to new research. It is citable and carries a permanent DOI. The final edited version will replace it automatically.